Theoretical and Experimental Studies of Water Complexes of *p*- and *o*-Aminobenzoic Acid

Yonggang He, Chengyin Wu, and Wei Kong*

Department of Chemistry, Oregon State University, Corvallis, Oregon 97331-4003

Received: December 6, 2004; In Final Form: January 18, 2005

We report studies of supersonically cooled water complexes of *p*- and *o*-aminobenzoic acid with one or two water molecules using two-color resonantly enhanced multiphoton ionization (REMPI) spectroscopy. Density functional theory calculations are carried out to identify structural minima of water complexes in the ground state. According to the calculation, water molecules are bound to both the C═O and -OH groups to form a cyclic hydrogen-bond network in the most stable isomer. Vibrational frequency calculations for the first electronically excited state of the most stable isomer agree well with the experimental observation. On the basis of this agreement, we believe that only one isomer exists in our molecular beam. The frequency shifts of a few normal modes caused by the water molecules further confirm the site of water addition. A surprising observation is that, for $OABA(H_2O)_n$ complexes, abundant intermolecular vibrational modes are clearly observable in the REMPI spectra, while for $PABA(H_2O)_n$ complexes, these modes are conspicuously missing. A red shift in the transition energy is observed for $OABA(H_2O)_1$, while blue shifts are observed for the rest of the complexes. This difference alludes to the relative stabilities of the water complexes of the two aminobenzoic acids in both the ground and excited electronic states. These observations will be discussed in comparison with those from the meta isomer.

Introduction

Studies of water-solvated organic chromophores containing competitive multiple hydrogen-bonding sites constitute an active area of research.[1−8] The importance of such studies lies in not only the fundamental nature of hydrogen bonding itself but also the understanding of the role of water in related processes such as catalysis, molecular recognition, and biochemical regulation.

Although the largest body of today's experimental data comes from studies in the condensed phase,[9] work in the gas phase can achieve investigations of hydrogen-bonding interactions in the absence of bulk solvent effects. Thus gas-phase studies can provide microscopic models in understanding a variety of interactions between the solute and solvent molecules. Molecular beam technology has proven an efficient way to prepare cold, isolated clusters of different sizes through supersonic jet expansion.[10] During the expansion, the vibrational and rotational degrees of freedom of the complexes are cooled. Interrogation with a variety of high-resolution spectroscopic methods such as resonantly enhanced multiphoton ionization (REMPI) and laser-induced fluorescence (LIF) can be achieved.

Interests in aminobenzoic acids arise from both their biological importance and their chemical properties. *o*-Aminobenzoic acid (OABA), also named anthranilic acid, has been used as a convenient fluorescence probe in internally quenched fluorescent peptides due to its high quantum yield and small size.[11,12] *p*-Aminobenzoic acid (PABA) is an antimetabolite of sulfanilamide and was once widely used as an active ingredient in sunscreen and a photodegradation inhibitor. PABA and OABA are both multifunctional hydrogen-bonding molecules. In protic solvents, they can act both as hydrogen atom acceptors, at the O atom of the C═O group and the N atom of the $-NH_2$ group, and as hydrogen atom donors at the −O−H and the H−N−H sites. They can also form a hydrogen bond through the aromatic π electrons. The existence of multiple hydrogen-bonding sites makes these molecules ideal models for studying the interaction between water and aromatic chromophores. The effect of water on the photophysical behaviors of these species is crucial in interpreting the message of the fluorescence probe.

Gas-phase spectroscopic investigations of PABA, OABA, and their water complexes have been carried out to a limited extent.[13−19] Using laser desorption, Meijer et al.[13] have recorded the REMPI spectra of bare PABA and its complexes with argon, methanol and water. However, no detailed vibrational assignment has been carried out. Southern et al.[14] have recorded the electronic and infrared spectra of bare OABA in a supersonic jet, and later, Stearns et al.[15] have extended the investigation to the corresponding water complexes. The emphasis of the work on OABA has been the dislocation of the hydrogen atom in the first electronically excited state (S_1), and the effect of the intramolecular hydrogen bond on water complexation. Our group has recently investigated the ground cationic state (D_0) of all three isomers of aminobenzoic acid using two-color zero kinetic energy (ZEKE) photoelectron spectroscopy.[16−18] We have achieved complete vibrational assignment of both the S_1 and the D_0 states. Our studies of the water complexes of the meta isomer (MABA) by use of REMPI and UV−UV hole-burning spectroscopic techniques have revealed the existence of multiple isomers of the bare molecule and the corresponding water complexes.[19] From the comparison between the observed vibrational frequency and our density functional theory (DFT) calculation, structural assignment and vibrational spectroscopy of the S_1 state have been achieved. Our observation of the change in the vibrational frequency and ionization threshold with the addition of water molecules has revealed a basic road map of water solvation.

The present report is a continuation of our study on water complexes of the different isomers of aminobenzoic acid.[19]

* Corresponding author: phone 541-737-6714; fax 541-737-2062; e-mail wei.kong@oregonstate.edu.

10.1021/jp0444565 CCC: $30.25
Published on Web 03/03/2005

Following the same procedure as used in our previous report, we present detailed vibrational assignment of the REMPI spectra of PABA$(H_2O)_n$ and OABA$(H_2O)_n$ complexes with n from 0 to 2. We have also performed quantum mechanical calculations to obtain structures and binding energies for possible isomers in the ground state and vibrational frequencies of these species in the first electronically excited state. These results will be discussed in comparison with our results on MABA, and the uniqueness of each isomer reflected from the spectroscopy of the solvent/solute complex will be explored.

Experimental Setup and Calculation Method

The experimental setup has been described elsewhere,[20,21] and the conditions for forming the water complexes of OABA and PABA are similar to those in the case of MABA.[19] Both one-color (1 + 1) and two-color (1 + 1′) REMPI experiments were performed to obtain vibrational information about the first excited state and the ionization energy (IE) of each complex. Mass-selected, one-color two-photon REMPI spectra of PABA$(H_2O)_{0-2}$ were recorded by scanning an optical parametric oscillator (OPO, Continuum, Panther, pumped by Continuum, Powerlite 7010) near the region of the S_1 state. The two-color two-photon REMPI spectra of OABA$(H_2O)_{0-2}$ were recorded by scanning a dye laser (Laser Analytical Systems, LDL 2051, pumped by Spectra Physics, GCR 230) through the vibronic levels of the S_1 state while another dye laser (Laser Analytical Systems, LDL 20505, pumped by Spectra Physics, GCR 190) was set at 285 nm for further ionization. To determine the ionization potential, we recorded the photoionization efficiency spectra (PIE) by fixing the OPO or one of the dye lasers at the origin of the S_1 state while scanning the second dye laser through the ionization threshold. In all two-laser experiments, the laser beams were set to counterpropagate, while the light path, the flight tube, and the molecular beam were mutually perpendicular. The resulting ions were accelerated by an extraction field of ~130 V/cm and detected by a chevron multichannel plate detector.

Possible structures of PABA, OABA, and their complexes with one (1:1 complex) or two (1:2 complex) water molecules were explored by performing a series of density functional theory (DFT) calculations by use of the Gaussian 98 and Gaussian 03 suites.[22,23] The procedure for generating and optimizing different water complexes was the same as that used in the case of MABA.[19] The most stable ground-state structures for both the 1:1 and 1:2 complexes were subsequently chosen as the starting point of optimization for the S_1 state at the CIS/6-31G level. Vibrational frequencies of the normal modes at the S_1 state were also calculated at the same level of theory. To obtain good agreement between theory and experiment in the vibrational assignment, a scaling factor of 0.95 was used for bare OABA, and a scaling factor of 0.9 was used for the rest of the compounds.[24]

Results

Theoretical Calculations: PABA$(H_2O)_{0-2}$. Our DFT optimization for the ground state of bare PABA at the B3LYP/6-31+G(d) level shows that PABA is nonplanar with an angle of 25.69° between the amino group and the plane of the ring. Exploration of isomer space minimum for the 1:1 complex at the B3LYP/6-31+G(d) level has led to the discovery of six stable isomers. The optimized structures together with their relative energies including zero-point vibrational energy (ZPVE) corrections are displayed in Figure 1. In general, these structures are similar to those of MABA, with the water molecule bound to the carboxyl pocket in the most stable isomer (I) to form a cyclic hydrogen-bond network. This isomer is lower in energy than the second most stable isomer (II) by 3.73 kcal/mol. This large energy difference implies that isomer I should be the dominant species in a supersonic jet. In the other higher energy isomers II−VI, only one hydrogen bond is formed, and on the basis of our previous experience, these structures are irrelevant to our experimental measurement.

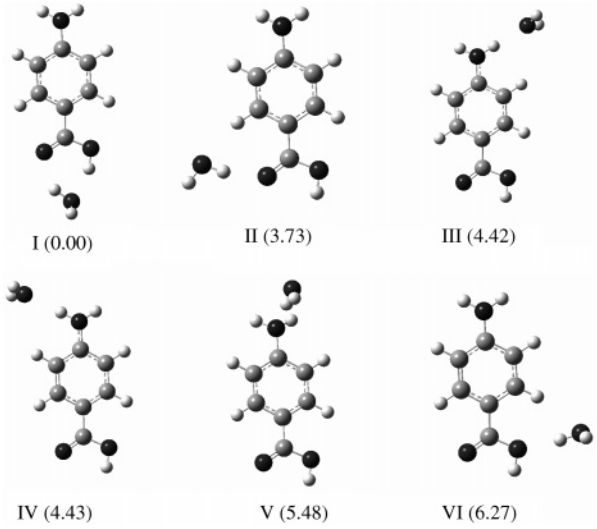

Figure 1. Optimized geometries of 1:1 water complex of PABA at the B3LYP/6-31+G(d) level. The values in parentheses are relative energies in kilocalories per mole.

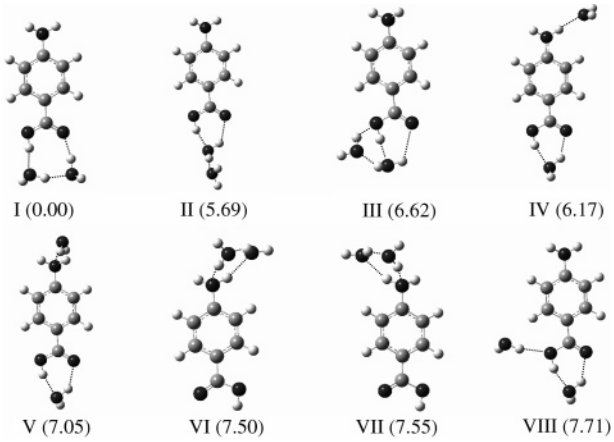

Figure 2. Optimized geometries of 1:2 water complex of PABA at the B3LYP/6-31+G(d) level. Values in parentheses are relative energies in kilocalories per mole.

Figure 2 shows eight of the most stable structures for the 1:2 complexes of PABA. Similar to the case of MABA, the energetically most stable structure incorporates three linear hydrogen bonds and allows each molecule to be both a donor and an acceptor. This structure can be viewed as a water dimer hydrogen-bonded to the C═O and the -OH group. Compared with the second most stable structure, in which only one water molecule interacts with the -COOH group, this structure is stable by 5.69 kcal/mol in energy. It should thus be the only possible species in our supersonic jet. It is interesting to notice that structure III has the maximum number of hydrogen bonds, but its bonding energy is much higher than structure I, even higher than structure IV with the two water molecules independent of each other.

Theoretical Calculations: OABA$(H_2O)_{0-2}$. Our DFT calculation on bare OABA at the B3LYP/6-31+G(d) level has resulted in two stable conformers, which agrees with the

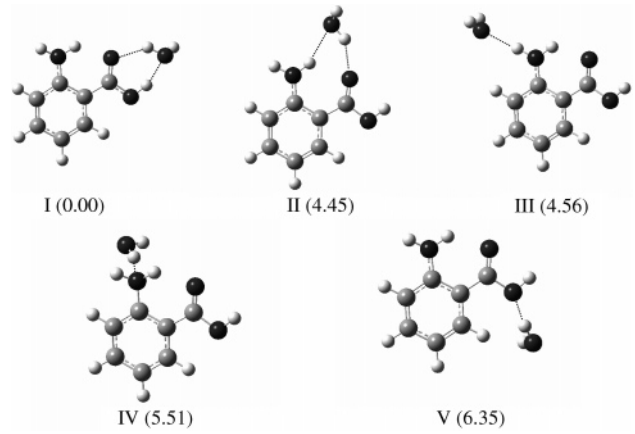

Figure 3. Optimized geometries of 1:1 water complex of OABA at the B3LYP/6-31+G(d) level. Values in parentheses are relative energies in kilocalories per mole.

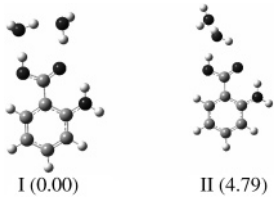

Figure 4. Two most stable geometries of the 1:2 water complex of OABA at the B3LYP/6-31+G(d) level. Values in parentheses are relative energies in kilocalories per mole.

calculation by Southern et al.[14] According to the hole-burning experiment by the original authors and our later experiment on both the S_1 and the D_0 state,[18] however, only the more stable isomer exists in a supersonic jet. In this structure, an intramolecular hydrogen bond is formed between one of the amino hydrogen atoms and the carbonyl group.

Adding one water molecule to the more stable structure of OABA has resulted in five stable structures, as depicted in Figure 3. In the most stable isomer I, water resides in pocket I according to Stearns et al.,[15] similar to the case of PABA$(H_2O)_1$. On the basis of the resonant ion-dip infrared spectroscopy (RIDIR) experiment,[15] this isomer should be the only species in the molecular beam. In isomer II, the water molecule bridges between the amino group and the carboxyl group. The formation of this isomer involves breaking of the intramolecular hydrogen bond between the two substituents and creation of two intermolecular bonds. Interestingly, the stability of isomers II and III is similar, although the number of hydrogen bonds are quite different. This is an indication of a high energy cost in breaking the intramolecular hydrogen bond.

The two most stable water complexes of OABA$(H_2O)_2$, shown in Figure 4, have similar structures as those in Figure 2. The most stable structure containing a six-membered ring in a cyclic hydrogen-bonding network has an additional binding energy of 4.79 kcal/mol compared to the next most stable isomer.

Summary of Theoretical Results. In summary, the bonding structures for PABA and OABA with water molecules are similar, and in all cases, only one dominant structure has been found. In the 1:1 complex, the water molecule resides in the pocket of the carboxyl group, and the stability of this structure is around 4 kcal/mol more than that of the next most stable one. In the 1:2 complex, a cyclic ring structure involving three hydrogen bonds is the most stable motif, with both water molecules bonded to the carboxyl group. Bonding at the amino site has proven costly in energy, even with the formation of a cyclic structure. The intermolecular hydrogen bond between two water molecules is stronger than that between a water molecule and the amino group. The intramolecular hydrogen bond in OABA does not seem to impose any influence on the intermolecular bond with water, at least for the most stable structure.

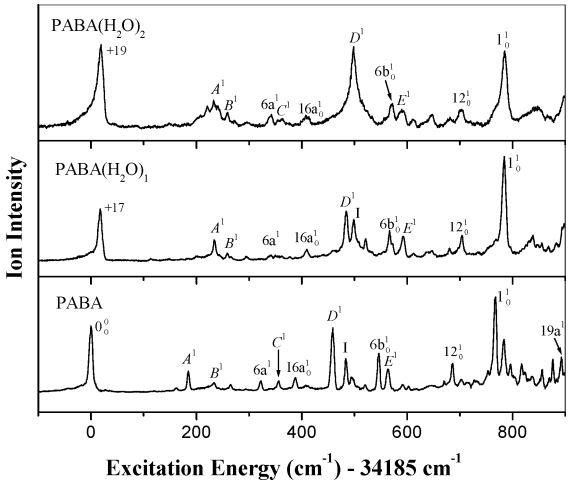

Figure 5. REMPI spectrum (1 + 1) of jet-cooled PABA$(H_2O)_n$ (n = 0−2) plotted with respect to the origin of the $S_1 \leftarrow S_0$ transition of bare PABA at 34 185 cm^{-1}.

Experimental Results: PABA$(H_2O)_{0-2}$. Figure 5 shows the one-color two-photon REMPI spectra of PABA$(H_2O)_{0-2}$ plotted with respect to the origin of the $S_1 \leftarrow S_0$ transition of bare PABA at 34 185 cm^{-1}. All three spectra demonstrate discrete narrowband structures. The one-color REMPI spectrum of bare PABA was first obtained by Meijer et al.[13] using laser desorption, and later, a complete vibrational assignment was achieved by our group based on ab initio and DFT calculations and in correlation with two-color zero kinetic energy photoelectron spectroscopy.[16] For both the 1:1 and 1:2 complexes, only one single strong transition near the origin is observable. This result is very different from those of water complexes of MABA where multiple origin bands were observed. Moreover, a striking similarity exists between the vibrational progression of both complexes as well as that of bare PABA; i.e., essentially all the major transitions observed in bare PABA are repeated in the spectra of the water complexes. These facts suggest that we are only observing a single conformation for each complex in the molecular beam, in agreement with our own calculation. Based on our hole-burning experiment on water complexes of MABA, even for an isomer with an additional instability of 3 kcal/mol, its contribution in our supersonic molecular beam was negligible. We therefore concluded that a hole-burning experiment on the water complexes of PABA was unnecessary.

The shifts of the origin band for both water complexes are small. The origin band of the 1:1 complex is blue-shifted by 17 cm^{-1} with respect to bare PABA, while the blue shift of the 1:2 complex is 19 cm^{-1}. These small spectral shifts indicate that the complexes are only slightly more stable in the S_0 state than in the S_1 state. In contrast, the shifts of the origin bands in water complexes of MABA were much larger, on the order of 100 cm^{-1} for the 1:1 complex.

A complete assignment of the observed vibronic transitions for all three species is listed in Table 1. Modes that are associated with the motion of the aromatic ring are labeled by the convention of Varsanyi's nomenclature.[25] Other modes that mainly involve the motion of the -NH_2 and -COOH moieties are named with letters from A to E in order of increasing frequency. An overall agreement between the calculation and the experiment is obtained when a scaling factor of 0.9 is used.[24]

TABLE 1: Observed Vibrational Frequencies and Assignments for the S_1 State of PABA$(H_2O)_{0-2}$

PABA		PABA$(H_2O)_1$		PABA$(H_2O)_2$		assignment and approximate description[b]
exp	calc[a]	exp	calc[a]	exp	calc[a]	
185	149	217	228	214	234	A_0^1, β(-COOH)
233	209	242	267	240	266	B_0^1, C-NH_2 torsion, β(-COOH)
322	323	323	343	323	351	$6a_0^1$, β(ring)
357	329			345	361	C_0^1, β(-NH_2)
388	376	392	389	389	389	$16a_0^1$, γ (ring)
459	466	467	480	479	483	D_0^1, β(-COOH), β(-NH_2)
483	512	481	484			I_0^1, NH_2 inversion
546	543	549	575	553	577	$6b_0^1$, β(ring)
564	564	576	584	570	585	E_0^1, -COOH scissoring, β(ring)
592		595				$B_0^1C_0^1$
687	694	687	707	684	709	12_0^1, β(ring)
768	767	767	772	766	773	1_0^1, ring breathing
784	762					$17b_0^1$, γ(ring)
796		838				$B_0^1E_0^1$
817						$C_0^1D_0^1$
857	906					$17a_0^1$, γ(ring)
876						$A_0^112_0^1$
893	936					$19a_0^1$, β(ring)

[a] Values include a scaling factor of 0.9. [b] β and γ represent in-plane bending and out-of-plane bending vibrations, respectively.

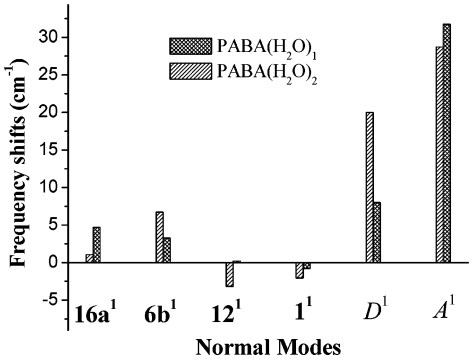

Figure 6. Frequency shifts of a few observed normal modes in PABA-$(H_2O)_n$ (n = 1, 2) relative to the bare compound. The uncertainty in the shift of mode D for PABA$(H_2O)_2$ is ~10 cm^{-1} due to the unresolved broad feature, while the uncertainty for the rest of the values is 3 cm^{-1}.

The observed frequency shifts for the water complexes compared with bare PABA are displayed in Figure 6. The $16a_0^1$ transition is observed at 388 cm^{-1} for bare PABA, while it occurs at 392 and 389 cm^{-1} for the 1:1 and 1:2 complexes, respectively. For modes 6b, 12, and 1, the frequencies in both complexes are also within a few wavenumbers of their respective values in the bare molecule. These modes mainly involve deformation of the aromatic ring, and with the addition of water molecules, they only undergo slight shifts. On the other hand, a large shift is observed for the in-plane bending mode of the carboxyl group: in Figure 6, mode A increases by ~30 cm^{-1} in both complexes. These experimental observations are also borne out from the theoretical calculations, as shown in Table 1, although the exact amount of frequency shift is even more dramatic in the calculation. The site of water addition should therefore be the carboxyl group for both n = 1 and 2, in excellent agreement with our DFT calculations. The shifts in other modes of the substituents are moderate, mainly because of their close coupling with the ring. For example, modes D and E involve collective motions of the whole molecular frame, while the displacement vectors of modes B and C undergo dramatic changes upon complexation. The in-plane bending motion of the -COOH moiety in mode B is frozen upon complexation. In mode *C*, the in-plane bending motion of the -NH_2 moiety extends to the water molecule(s) in the complex-(es). Interestingly, the addition of the second water molecule

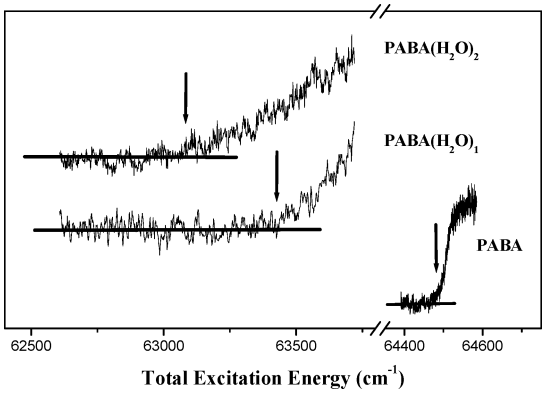

Figure 7. Two-color PIE spectra of jet-cooled PABA$(H_2O)_n$ (n = 0−2). IE values are marked by an arrow on each trace.

to the 1:1 complex results in marginal changes in the vibrational frequency. This fact suggests that the second water molecule should be in close proximity to the first water molecule, exerting minimal disturbance to the molecular frame.

To determine the ionization potential, we have recorded the photoionization efficiency spectra for all three complexes in a two-color two-photon ionization experiment. Figure 7 shows the threshold portion of the PIE spectrum obtained by pumping to the origin of the S_1 state of each species and scanning the probe laser. The ionization potential has been obtained by linearly extrapolating the post-threshold portion to the baseline of the ion signal. Taking into account the field ionization effect in the ion collection region,[26] the threshold for bare PABA has been determined to be 8.001 eV, in good agreement with our own value obtained from a ZEKE experiment.[16] In contrast to the sharp onset of ion signal at the threshold of bare PABA, ions with n = 1 and 2 have shallow slopes near the threshold, typical for water complexes of aromatic molecules. By use of the same linear extrapolation method, the IEs for the 1:1 and the 1:2 complexes have been determined to be 7.871 and 7.823 eV respectively. Due to the shallow slopes around the ionization threshold in Figure 7, the uncertainty in these values is estimated to be 0.01 eV. The shallow slopes also indicate substantial geometry changes of the complex upon ionization. Limited by the signal-to-noise ratio and the small FC factors at the threshold, unfortunately, we were unsuccessful in recording the ZEKE spectra of the complexes. The vibrational information from such an experiment would shed more light on the change in geometry upon ionization. On the other hand, the state selection offered in the first step of excitation has eliminated contributions from hot bands, and the threshold obtained from the current extrapolation method is therefore of a higher precision compared with that from single-photon ionization. Interestingly, using a logarithmic fitting method,[27] we arrived at the same values within our error limit, and this fact further demonstrates the advantage of state selection.

Experimental Results: OABA$(H_2O)_{0-2}$. Figure 8 displays the two-color two-photon REMPI spectra of OABA$(H_2O)_{0-2}$ plotted with respect to the origin of bare OABA at 28594 cm^{-1}. These spectra are similar to those reported by Stearns et al.[15] in terms of the shift in origin for both complexes and the distribution of active vibrational modes. In this work, we have extended the measurement more than 400 cm^{-1} beyond that reported by Stearns et al.,[15] and we have also attempted a complete assignment of all the observed vibronic features for both complexes. In Figure 8, all three spectra demonstrate discrete narrow-band structures, and the similarities among them are marginal. Both observations indicate that the smaller

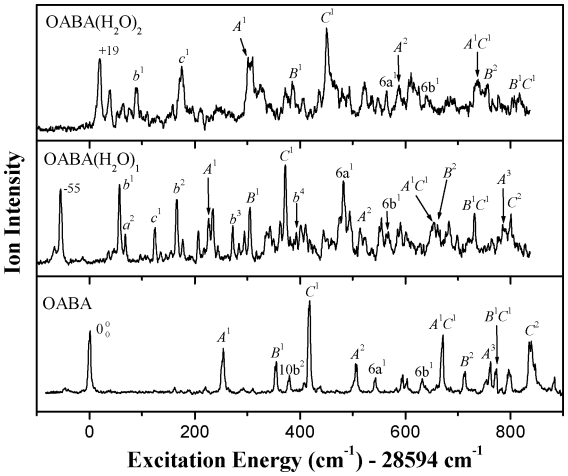

Figure 8. REMPI spectrum (1 + 1′) of jet-cooled OABA$(H_2O)_n$ (n = 0−2) plotted with respect to the origin of the $S_1 \leftarrow S_0$ transition of bare OABA at 28 594 cm^{-1}.

complexes are not a product of dissociation from the larger complexes. The lowest energy transition for the 1:1 complex is red-shifted by 55 cm^{-1} with respect to the bare molecule, and this band is assigned as the origin band. In contrast, a blue shift of 19 cm^{-1} is observed in the REMPI spectrum of the 1:2 complex. Using resonant ion-dip infrared spectroscopy, Stearns et al.[15] have established that there is only one dominant isomer in the 1:1 complex; thus a UV−UV hole burning experiment is deemed unnecessary. Although a small shoulder to the red edge of the origin band in trace b is observable in our spectrum, perhaps due to the higher temperature of our molecular beam compared with that of Stearns et al.,[15] given its low intensity and our experience with hole-burning spectroscopy in water complexes of MABA, a hole-burning experiment could, at best, only identify the existence of a minor isomer, with no vibrational information. For the 1:2 complex, both our calculation result on the binding energy difference among the possible isomers (Figure 4) and the assignment of the observed vibrational modes as listed in Table 2 imply the existence of only one isomer. Limited by the signal strength of the spectrum, we were unable to perform a hole-burning experiment to confirm this assumption.

A complete assignment of the observed vibronic transitions for all three species is listed in Table 2. Also listed in the table are our own calculations at the CIS/6-31G(d) level for the monomer and at the CIS/6-31G level for the water complexes. Due to the different levels of calculation, we have used different scaling factors: 0.95 for the bare molecule and 0.9 for the complexes. The same nomenclature as that applied for PABA$(H_2O)_{0-2}$ is used in this table. For the intermolecular modes, we use lowercase alphabets in the order of increasing frequency for the 1:1 complex, and to make the comparison intuitive between the two complexes, we use the same name for those in the 1:2 complex if the displacement vectors are similar in the two complexes. Other observed intermolecular modes that are unique to the 1:2 complex are only listed in Table 2. Our assignment is in overall agreement with that of Stearns et al.,[15] except for the in-plane bending mode B of the -COOH moiety. Stearns et al.[15] assigned the transition at 288 cm^{-1} in OABA$(H_2O)_1$ as mode B on the basis of its similar position and intensity as that of the monomer. We believe that this peak belongs to the combination of modes b and c. We assign the peak at 281 cm^{-1} as mode B, consistent with the value of 282 cm^{-1} from the CIS calculation. Moreover, this assignment makes it more reasonable to assign the transitions

TABLE 2: Observed Vibrational Frequencies and Assignments for the S_1 State of OABA$(H_2O)_{0-2}$

OABA		OABA$(H_2O)_1$		OABA$(H_2O)_2$		assignment and
exp	calc[a]	exp	calc[b]	exp	calc[b]	approximate description[c]
				20	24	γ(H_2O−ring)
				45	46	γ(H_2O−ring)
		111	118	70	83	b_0^1, β(H_2O−ring)
		123	112			a_0^2, γ(H_2O−ring)
		180	180	156	171	c_0^1, ν(H_2O−ring)
220		210				A_0^2, C−COOH torsion
		221		139		b_0^2
		232				$a_0^2b_0^1$
254	258	281	282	287	298	B_0^1, β(-COOH)
		288				$b_0^1c_0^1$
		299				$a_0^2c_0^1$
				306		c_0^2
		328				b_0^3
		339	334			$16a_0^1$, γ (ring)
		349				$a_0^2b_0^2$
355	371	360	371	366	380	C_0^1, β(-NH_2)
		391		353		$b_0^1B_0^1$
379	416	398	430	388	430	$10b_0^2$, γ(ring) and NH_2 wag
418	415	427	432	431	414	D_0^1, β(-NH_2), β(-COOH)
		448				b_0^4
		466	467	475	481	d_0^1, β(H_2O−ring)
		499				$b_0^2B_0^1$
				503		$b_0^1D_0^1$
				518		$c_0^1C_0^1$
		549				$a_0^2D_0^1$
506		569		569		B_0^2
544	560	537	548	546	548	$6a_0^1$, β(ring)
595						$A_0^210b_0^2$
602	603	579	586	592	585	$16b_0^1$, γ (ring)
		610				$b_0^3B_0^1$
632	626	622	608	620	606	$6b_0^1$, β(ring)
		646				$B_0^1C_0^1$
		656				$b_0^2D_0^1$
672		709		719		$B_0^1D_0^1$
713		716		737		C_0^2
		738				$B_0^1a_0^2b_0^3$
		753				$b_0^3D_0^1$
762		840				B_0^3
772		787		798		$C_0^1D_0^1$
797		818				$B_0^16a_0^1$
884	875	831	842			$19a_0^1$, β(ring)
839		856				D_0^2

[a] Values include a scaling factor of 0.95. [b] Values include a scaling factor of 0.9. [c] ν, β, and γ represent stretching, in-plane bending, and out-of-plane bending vibrations, respectively.

at 569 and 840 cm^{-1} to overtones of mode B and peaks at 391, 646, 709, and 818 cm^{-1} to its combination bands. It is worth noting that, for both complexes, there are many more low-frequency modes than listed in Table 2 on the basis of our calculation. The two features at 20 and 46 cm^{-1} in the spectrum of the 1:2 complex are most likely out-of-plane intermolecular vibrations among the three constituents as listed in Table 2. Although indirect, this assignment of all the major features in the low-frequency region of the spectrum further confirms the assumption that there are no other isomers in the molecular beam for the water complexes of OABA.

Unlike the REMPI spectra of PABA complexes shown in Figure 5, Figure 8 displays rich activities of intermolecular vibration for both the 1:1 and 1:2 complexes. In the spectrum of the 1:1 complex, a strong transition at 111 cm^{-1} is assigned as the in-plane bending mode b. This mode is so active that a clear vibrational progression with v up to 4 is observable, where v is the vibrational quantum number. Two other strong features at 123 and 180 cm^{-1} are assigned as the out-of-plane bending mode a with $\Delta v = 2$ and the fundamental transition of a stretching mode c. Modes b and c are also observed for the 1:2

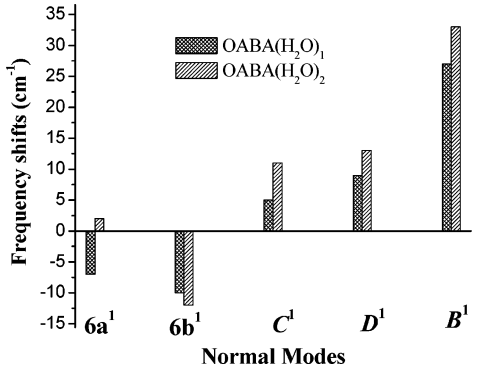

Figure 9. Frequency shifts of a few observed normal modes in OABA-$(H_2O)_n$ ($n = 1, 2$) relative to the bare compound. The uncertainty for all the values is 3 cm^{-1}.

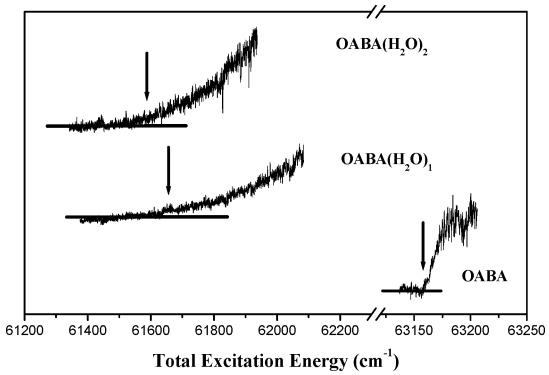

Figure 10. Two-color PIE spectra of jet-cooled OABA$(H_2O)_n$ ($n = 0-2$). IE values are marked by an arrow on each trace.

complex of OABA at 70 and 156 cm^{-1}, respectively. The obvious shifts in both the inter- and intramolecular vibrational modes among the three species further reinforce the assessment that the smaller complexes are not dissociative products of the larger complexes.

The shifts in frequency for some of the observed modes in the water complexes of OABA are displayed in Figure 9. Similar to the case of PABA, the ring deformation mode 6a changes by less than 10 cm^{-1}, while the in-plane bending mode B of the carboxyl group increases by $\sim$30 cm^{-1}. The site of water addition should therefore be the carboxyl group, in excellent agreement with our theoretical predictions. Modes C and D involve collective motions of the whole molecular frame and are therefore not as sensitive as mode B to the addition of water.

Figure 10 shows the threshold portion of the PIE spectra for all three species. The threshold for bare OABA has been determined to be 7.836 eV from this procedure, and this value is in good agreement with our own report from a ZEKE experiment.[18] The IEs for the 1:1 and the 1:2 complexes have been determined to be 7.644 and 7.635 eV, respectively. Similar to the situation of the water complexes of PABA, the onset of the ion signal for the water complexes of OABA is also quite slow with the increase of excitation energy.

Discussion

The above experimental and theoretical results provide a consistent picture with regard to the initial step of water solvation of aminobenzoic acids. All aminobenzoic acids can be viewed as electron "push−pull" molecules, and in the ground state, a fraction of the electron from the amino group is transferred to the carboxyl group. The lack of electrons on the amino group and the ready availability of extra electrons on the carboxyl group therefore result in an amphipathic behavior in both molecules. For MABA,[19] due to the weaker electron induction effect in meta substitution, minor isomers in both the 1:1 and the 1:2 complexes were observed, while for PABA and OABA, our observation and that of Stearns et al.[15] both allude to the existence of only one isomer in all cases. We therefore conclude that it is the hydrogen-bond site on the carboxyl group that the water molecules prefer to occupy. The amino group loses out in the competition even with the availability of two water molecules.

TABLE 3: Calculated Hydrogen Bond Lengths in the 1:1 Complex of PABA and OABA upon Electronic Excitation

	C═O···HO_w (Å)		O−H···OH_w (Å)	
	S_0	S_1	S_0	S_1
PABA$(H_2O)_1$	1.914	2.018	1.803	1.942
OABA$(H_2O)_1$	1.943	1.902	1.790	1.798

Unique to OABA is the intramolecular hydrogen bond between the two substituents, and on the basis of our results, this hydrogen bond has minimal effect on the water complexes. In the study of Stearns et al.,[15] the "free" NH stretching vibration in the S_1 state of OABA$(H_2O)_1$ was the same as that of bare OABA. The authors thus concluded that water complexation exerts only a minor perturbation to the molecular frame. Our study is sensitive to the in-plane bending mode C of the amino group, and as seen in Table 2, only a slight shift of this mode, on the order of 10 cm^{-1}, is observable. This result is in agreement with the study of Stearns et al.[15]

One of the intriguing results from the above measurement is that, except for the 1:1 complex of OABA, the 1:2 complex of OABA and both water complexes of PABA demonstrate blue shifts. The spectra of the water complexes of MABA, interestingly, all demonstrated sizable red shifts.[19] These shifts reflect the difference of the ground and the excited state in water complexation. Typically, a blue shift implies a more tightly bound ground state than the excited state, and vice versa. It would thus be instructive to compare the geometry changes upon excitation. The location of the water molecules is the same for OABA and PABA in both water complexes. Table 3 lists the hydrogen-bond lengths for the 1:1 complexes. Upon electronic excitation, the lengths for both hydrogen bonds C═O···HO_w and O−H···O_w *increase* in the 1:1 complex of PABA, implying a decrease in bond strength. In contrast, the bond length for C═O···HO_w *decreases* in OABA$(H_2O)_1$, indicating a slight enhancement of the hydrogen bond. This additional stability in the S_1 state of OABA$(H_2O)_1$ may be the reason for the red shift of the origin band. Unfortunately, the precision from our calculation on the binding energy is insufficient to confirm the above assessment with regard to the relative strength of hydrogen bonding. The blue shift of the 1:2 complex of OABA, on the other hand, demonstrates the intricate balance between the inter- and intramolecular hydrogen bonds in the S_0 and S_1 states.

Another intriguing result is the missing intermolecular modes in the spectra of the water complexes of PABA in Figure 5. On the basis of our calculation, these modes should appear within 200 cm^{-1} above the origin band. Our initial suspicion is small Franck−Condon factors near the origin of the electronic transition, since upon excitation, one of the OH bond in water rotates into the plane of the aromatic ring. However, the existence of the large origin band dismisses this possibility. An opposite extreme is that there is no change in the displacement vector upon excitation, and the only nonvanishing vibrational band is thus the origin band. It is interesting to note that our

TABLE 4: Ionization Energies[a] of PABA(H_2O)$_n$ and OABA(H_2O)$_n$

n	PABA	OABA
0	8.001	7.836
1	7.871	7.644
2	7.823	7.635

[a] Ionization energies are given in electronvolts.

spectroscopic assignment of the water complexes of MABA did not reveal the existence of intermolecular vibrational modes either. The prevalence of the rich intermolecular features in the spectra of the water complexes of OABA is therefore unique to the ortho isomer. The change in balance between the inter- and intramolecular hydrogen bond during electronic excitation may have contributed to the activation of the intermolecular vibrational modes in the water complexes of OABA.

Table 4 lists the IE values for both isomers and their water complexes. On the basis of our previous observation, the intramolecular hydrogen bond in OABA is stronger in the cation than in the neutral molecule, and this extra stability is reflected in the smaller IE value for OABA.[18] The differences between the IE values of the PABA and OABA complexes containing the same number of water molecules are on the order of 0.2 eV, similar to that of the bare molecules.[16,18] The intramolecular hydrogen bond has therefore a negligible effect on water complexation, consistent with previous observations.[15] For both isomers, the addition of water molecules stabilizes the cationic state, and red shifts of 0.130 and 0.192 eV are observable for the 1:1 complexes. The addition of a second water molecule, in contrast, has a much smaller effect. This observation is consistent with the formation of a water cluster within the carboxyl group.

Conclusion

Spectroscopic properties of the excited state of PABA and OABA water complexes have been studied by two-color resonantly enhanced multiphoton ionization spectroscopy. Structures and binding energies for several of the possible isomers in the ground state have been explored based on DFT calculations. In all cases, only the most stable isomer exists in the supersonic molecular beam, and the intramolecular hydrogen bond in OABA has minimal effect on water complexation. With the aid of ab initio calculations, vibrational modes of the S_1 state of the most stable complexes have been assigned, and a reasonable agreement between theory and experiment has been obtained. From the frequency shifts of some of the observed normal modes upon water addition, we conclude that it is the hydrogen-bond sites on the carboxyl group that the water molecules prefer to occupy. The ionization thresholds of both bare molecules and their water complexes have been determined, although with a larger uncertainty for the water complexes than for the bare molecules due to the shallow slope in the corresponding PIE spectra.

Acknowledgment. This work was supported by the National Science Foundation, Division of Chemistry. Acknowledgment is made to the donors of the Petroleum Research Fund, administered by the American Chemical Society, for partial support of this research. W.K. is an Alfred P. Sloan research fellow.

References and Notes

(1) Bernstein, E. R. *Atomic and Molecular Clusters*; Elsevier: Amsterdam, 1990.

(2) Jeffrey, G. A.; Saenger, W. *Hydrogen Bonding in Biological Structures*; Springer: Berlin, 1991.

(3) Castleman, A. W., Jr.; Wei, S. *Annu. Rev. Phys. Chem.* **1994**, *45*, 685−719.

(4) Zwier, T. S. *Annu. Rev. Phys. Chem.* **1996**, *47*, 205−241.

(5) Wolfenden, R.; Snider, M. J. *Acc. Chem. Res.* **2001**, *34*, 938−945.

(6) Robertson, E. G.; Simons, J. P. *Phys. Chem. Chem. Phys.* **2001**, *3*, 1−18.

(7) Neusser, H. J.; Siglow, K. *Chem. Rev.* **2000**, *100*, 3921−3942.

(8) Brutschy, B. *Chem. Rev.* **2000**, *100*, 3891−3920.

(9) Jeffrey, G. A. *An Introduction to Hydrogen Bonding*; Oxford University Press: New York, 1997.

(10) *Atomic and Molecular Beam Methods*; Scoles, G., Ed.; Oxford University Press: New York, 1988; Vol. 1.

(11) Turchilleo, R. F.; Lamy-Freund, M. T.; Hirata, I. Y.; Juliano, L.; Ito, A. S. *Biophys. Chem.* **1998**, *73*, 217−225.

(12) Ito, A. S.; Turchilleo, R. F.; Hirata, I. Y.; Cezari, M. H. S.; Meldal, M.; Juliano, L. *Biospectroscopy* **1998**, *4*, 395−402.

(13) Meijer, G.; de Vries, M. S.; Hunziker, H. E.; Wendt, H. R. *J. Chem. Phys.* **1990**, *92*, 7625−7635.

(14) Southern, C. A.; Levy, D. H.; Florio, G. M.; Longarte, A.; Zwier, T. S. *J. Phys. Chem. A* **2003**, *107*, 4032−4040.

(15) Stearns, J. A.; Das, A.; Zwier, T. S. *Phys. Chem. Chem. Phys.* **2004**, *6*, 2605−2610.

(16) He, Y.; Wu, C.; Kong, W. *J. Chem. Phys.* **2004**, *121*, 3533−3539.

(17) He, Y.; Wu, C.; Kong, W. *J. Chem. Phys.* **2004**, *121*, 8321−8328.

(18) Wu, C.; He, Y.; Kong, W. *Chem. Phys. Lett.* **2004**, *398*, 351−356.

(19) He, Y.; Wu, C.; Kong, W. *J. Phys. Chem. A* **2005**, *109*, 748−753.

(20) He, Y.; Wu, C.; Kong, W. *J. Phys. Chem. A* **2003**, *107*, 5145−5148.

(21) He, Y.; Wu, C.; Kong, W. *J. Phys. Chem. A* **2004**, *108*, 943−949.

(22) Frisch, M. J.; Trucks, G. W.; Schlegel, H. B.; Scuseria, G. E.; Robb, M. A.; Cheeseman, J. R.; Zakrzewski, V. G.; Montgomery, J. A., Jr.; Stratmann, R. E.; Burant, J. C.; Dapprich, S.; Millam, J. M.; Daniels, A. D.; Kudin, K. N.; Strain, M. C.; Farkas, O.; Tomasi, J.; Barone, V.; Cossi, M.; Cammi, R.; Mennucci, B.; Pomelli, C.; Adamo, C.; Clifford, S.; Ochterski, J.; Petersson, G. A.; Ayala, P. Y.; Cui, Q.; Morokuma, K.; Malick, D. K.; Rabuck, A. D.; Raghavachari, K.; Foresman, J. B.; Cioslowski, J.; Ortiz, J. V.; Stefanov, B. B.; Liu, G.; Liashenko, A.; Piskorz, P.; Komaromi, I.; Gomperts, R.; Martin, R. L.; Fox, D. J.; Keith, T.; Al-Laham, M. A.; Peng, C. Y.; Nanayakkara, A.; Gonzalez, C.; Challacombe, M.; Gill, P. M. W.; Johnson, B. G.; Chen, W.; Wong, M. W.; Andres, J. L.; Head-Gordon, M.; Replogle, E. S.; Pople, J. A. *Gaussian 98*, revision A.7; Gaussian, Inc.: Pittsburgh, PA, 1998.

(23) Frisch, M. J.; Trucks, G. W.; Schlegel, H. B.; Scuseria, G. E.; Robb, M. A.; Cheeseman, J. R.; Montgomery, J. A., Jr.; Vreven, T.; Kudin, K. N.; Burant, J. C.; Millam, J. M.; Iyengar, S. S.; Tomasi, J.; Barone, V.; Mennucci, B.; Cossi, M.; Scalmani, G.; Rega, N.; Petersson, G. A.; Nakatsuji, H.; Hada, M.; Ehara, M.; Toyota, K.; Fukuda, R.; Hasegawa, J.; Ishida, M.; Nakajima, T.; Honda, Y.; Kitao, O.; Nakai, H.; Klene, M.; Li, X.; Knox, J. E.; Hratchian, H. P.; Cross, J. B.; Adamo, C.; Jaramillo, J.; Gomperts, R.; Stratmann, R. E.; Yazyev, O.; Austin, A. J.; Cammi, R.; Pomelli, C.; Ochterski, J. W.; Ayala, P. Y.; Morokuma, K.; Voth, G. A.; Salvador, P.; Dannenberg, J. J.; Zakrzewski, V. G.; Dapprich, S.; Daniels, A. D.; Strain, M. C.; Farkas, O.; Malick, D. K.; Rabuck, A. D.; Raghavachari, K.; Foresman, J. B.; Ortiz, J. V.; Cui, Q.; Baboul, A. G.; Clifford, S.; Cioslowski, J.; Stefanov, B. B.; Liu, G.; Liashenko, A.; Piskorz, P.; Komaromi, I.; Martin, R. L.; Fox, D. J.; Keith, T.; Al-Laham, M. A.; Peng, C. Y.; Nanayakkara, A.; Challacombe, M.; Gill, P. M. W.; Johnson, B.; Chen, W.; Wong, M. W.; Gonzalez, C.; Pople, J. A. *Gaussian 03*, revision A.1; Gaussian, Inc.: Pittsburgh, PA, 2003.

(24) Casida, M. E.; Jamorski, C.; Casida, K. C.; Sulahub, D. R. *J. Chem. Phys.* **1998**, *108*, 4439−4449.

(25) Varsanyi, G. *Assignment of Vibrational Spectra of Seven Hundred Benzene Derivatives*; Wiley: New York, 1974.

(26) Duncan, M. A.; Dietz, T. G.; Smalley, R. E. *J. Chem. Phys.* **1981**, *75*, 2118−2125.

(27) Kappes, M. M.; Schär, M.; Röthlisberger, U.; Yeretzian, C.; Schumacher, E. *Chem. Phys. Lett.* **1988**, *143*, 251−258.